Active-Site pKa Determination for Photoactive Yellow Protein Rationalizes Slow Ground-State Recovery

Oktaviani, Nur Alia; Pool, Trijntje J.; Yoshimura, Yuichi; Kamikubo, Hironari; Scheek, Ruud M.; Kataoka, Mikio; Mulder, Frans A. A.

Published in:
Biophysical Journal

DOI:
10.1016/j.bpj.2017.04.008

Biophysical Journal
Article

Biophysical Society

Active-Site pKa Determination for Photoactive Yellow Protein Rationalizes Slow Ground-State Recovery

Nur Alia Oktaviani,[1] Trijntje J. Pool,[1] Yuichi Yoshimura,[2] Hironari Kamikubo,[3] Ruud M. Scheek,[1] Mikio Kataoka,[3] and Frans A. A. Mulder[1,2,*]

[1]Groningen Biomolecular Sciences and Biotechnology Institute, University of Groningen, Nijenborgh, Groningen, the Netherlands; [2]Interdisciplinary Nanoscience Center (iNANO) and Department of Chemistry, Aarhus University, Aarhus, Denmark; and [3]Graduate School of Materials Science, Nara Institute of Science and Technology, Ikoma, Japan

ABSTRACT The ability to avoid blue-light radiation is crucial for bacteria to survive. In *Halorhodospira halophila*, the putative receptor for this response is known as photoactive yellow protein (PYP). Its response to blue light is mediated by changes in the optical properties of the chromophore *para*-coumaric acid (*p*CA) in the protein active site. PYP displays photocycle kinetics with a strong pH dependence for ground-state recovery, which has remained enigmatic. To resolve this problem, a comprehensive pK_a determination of the active-site residues of PYP is required. Herein, we show that Glu-46 stays protonated from pH 3.4 to pH 11.4 in the ground (pG) state. This conclusion is supported by the observed hydrogen-bonded protons between Glu-46 and *p*CA and Tyr-42 and *p*CA, which are persistent over the entire pH range. Our experimental results show that none of the active-site residues of PYP undergo pH-induced changes in the pG state. Ineluctably, the pH dependence of pG recovery is linked to conformational change that is dependent upon the population of the relevant protonation state of Glu-46 and the *p*CA chromophore in the excited state, collaterally explaining why pG recovery is slow.

INTRODUCTION

Photoactive yellow protein (PYP) is a small (14 kDa) soluble protein from the negative phototactic bacterium *Halorhodospira halophila*. The absorption spectrum of PYP correlates perfectly with the wavelength dependence of the phototactic response, and hence, PYP has been suggested to serve as the photoreceptor for negative phototaxis (1). PYP contains 125 amino acids (aa), which form a sheet of six antiparallel β-strands flanked by five α-helices in an α/β-fold. High-resolution structures of PYP have been determined by x-ray and neutron crystallography and NMR spectroscopy (2–4). The chromophore of PYP, *para*-coumaric acid (*p*CA), is buried in the hydrophobic core of the protein and forms a covalent thioester bond to Cys-69 and two short hydrogen bonds with Tyr-42 and Glu-46. Early studies suggested, based on absorption spectroscopy (5,6), Raman spectroscopy (7), and x-ray crystallography (5), that the *p*CA chromophore is present as a phenolate anion in the pG state. However, more recently, joint refinement of x-ray and neutron crystallography diffraction data showed that the deuterium is shared between Glu-46 and *p*CA, suggesting that the negative charge is delocalized by resonance comprising both π-conjugated groups (4). Furthermore, the backbone atoms of Cys-69 are involved in hydrogen bonds to the side-chain atoms of Tyr-94 and Ser-72 (Fig. 1). Arg-52 is considered to function as a gate to the active center of PYP, causing solvent exposure and protonation of the chromophore upon opening (8).

Upon blue-light irradiation, absorption of a photon triggers the *trans*-to-*cis* isomerization of the *p*CA cofactor on the picosecond timescale (9). This process is followed by dissociation of the N-terminal region from its Per-Arnt-Sim domain and proton transfer, leading to breakage of the unusually short hydrogen bond between *p*CA and Glu-46. As a consequence, the active site becomes exposed to the solvent and *p*CA becomes protonated. This state is known as the pB (excited) or PYP_M state. The wavelength where *p*CA absorption is at a maximum changes from 446 nm in the ground (pG) state to 355 nm in the pB state (3,10). Finally, the partially folded form of PYP in the pB state relaxes back in the pG state, which is characterized by

Submitted December 23, 2016, and accepted for publication April 10, 2017.

*Correspondence: fmulder@chem.au.dk

Editor: Jeff Peng.

http://dx.doi.org/10.1016/j.bpj.2017.04.008

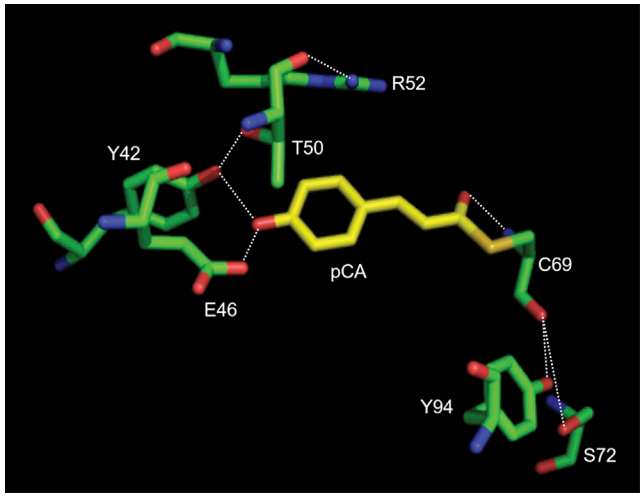

FIGURE 1 Hydrogen-bonding network in the active site of PYP, PDB: 2ZOI (4). To see this figure in color, go online.

formation of the central β-sheet and consolidation of residues close to *p*CA on the second timescale (3).

During the steps in this photocycle, PYP undergoes a sequence of structural changes, and the timescale for recovery of the pG state displays a strong pH dependence (11–13): The recovery rate from pB to pG exhibits a bell-shaped curve with a maximum at pH 7.9. The p*K* values extracted from that curve are 6.4 and 9.4, indicating that protonation and deprotonation of two groups is involved (14). When Glu-46 is mutated to Gln, the recovery-rate curve changes from bell-shaped to sigmoidal, and the maximal rate is increased by two orders of magnitude. The extracted p*K* value from that curve is 8 (14).

One theoretical study put forward that in the pB state, the pK_a values for Glu-46 and chromophore *p*CA are 6.37 and 9.35, respectively (15). In that study, it was suggested that the extracted p*K* constants from the bell-shaped curve of Genick et al. (14) correspond to the pK_a constants of Glu-46 and *p*CA in the pB state (15). In pB at low pH, Glu-46 and *p*CA are predominantly in their protonated form, which causes slow recovery from pB to pG, as Glu-46 needs to become deprotonated. As the pH increases, the fraction of deprotonated Glu-46 increases, and this accelerates the recovery rate. However, above pH 7.9, recovery again becomes slow, as now the productive fraction of protonated *p*CA rapidly decreases. In contrast, in a recent quantum mechanics/molecular mechanics study, pK_a constants for Glu-46 and *p*CA in pG were calculated to be 8.6 and 5.4, respectively (16), at variance with previous studies (17,18) and implying that the pH dependence of recovery would also depend on proton affinities in pG.

Unfortunately, until now, residue-specific experimental determination of active-site protonation states and pK_a constants for PYP was lacking, so that it cannot be concluded to what extent the pH dependence of photocycle pB-state recovery is due to protonation/deprotonation that occurs in the pG or pB state.

NMR spectroscopy is the most reliable method for determining the protonation state of individual titratable groups in proteins (19). Several two-dimensional (2D) NMR experiments have been developed to determine the individual side-chain pK_a constants for His, Asp, Glu, Tyr, Lys, and Arg in proteins (19–25). In this study, we present a comprehensive side-chain pK_a determination of titratable groups in the PYP active site by NMR. Our results demonstrate that none of the groups around the active site change protonation state in the pG state over the pH interval from 3.4 to 11.4. However, the pH dependence of PYP in the photocycle can be adequately explained by a pH dependence of the active-site residues in the pB state.

MATERIAL AND METHODS

Sample preparation

Uniformly [^{13}C,^{15}N]-labeled PYP was produced in M9 minimal medium containing ^{13}C glucose and $^{15}NH_4Cl$ and was purified as described previously (26). NMR samples contained ~1.0 mM PYP, 0.15 mM 4,4-dimethyl-4-silapentane-1-sulfonate, and 10% D_2O. Buffers containing 5 mM phosphate, 15 mM sodium (bi)carbonate, or 15 mM sodium acetate-d_3 were used for the pH ranges 5.9–9.2, 8.6–11.4 and 3.4–5.8, respectively. The pH was changed in steps of 0.2 pH units by adding a few μL of HCl or NaOH solution. For calibrating the pH meter in the range pH 4–10, calibration buffers of pH 4.0, 7.0, and 10.0 were used; for calibrating the pH meter in the pH range 1.0–4.0, a 0.10 M HCl solution and a calibration buffer of pH 4 were used; For calibrating the pH meter in the range pH 10–12, 10 mM NaOH and a calibration buffer of pH 10 were used.

NMR experiments

Unless specified otherwise, all 1D ^{1}H, 2D, and 3D NMR experiments were carried out at 293 K using a Varian Unity INOVA 600 MHz spectrometer equipped with a triple-resonance field-gradient probe. For experimental settings, see the Supporting Material. The 2D and 3D NMR data were processed using NMRPipe (27), and the spectra were analyzed using Sparky (28). All chemical shifts were referenced to 4,4-dimethyl-4-silapentane-1-sulfonate according to the recommendation of the International Union of Pure and Applied Chemistry (29).

Assignment of the Tyr-42 hydroxyl proton signal

The phenolic hydroxyl proton of Tyr-42 was assigned using a long-range ^{1}H-^{13}C correlation experiment, as shown in Fig. 2. The spectrum for uniformly [^{13}C,^{15}N]-labeled PYP at pH 6.2 was recorded at 288 K on a Bruker (Billerica, MA) Avance III 950 MHz spectrometer equipped with a TCI cryogenic probe head. The spectral widths were 22.7 kHz (23.9 ppm) and 19.1 kHz (80.0 ppm) for ^{1}H and ^{13}C, respectively. The ^{1}H and ^{13}C carrier frequencies were placed at 4.89 and 122.8 ppm, respectively. The spectrum was collected with 768 (^{1}H, t_2) × 56 (^{13}C, t_1) complex points. In the pulse sequence, the narrow and wide bars represent 90 and 180° pulses, respectively. Unless otherwise indicated, the pulses are applied with phase *x*. Water flip-back pulses for a duration of 1 ms to selectively rotate the magnetization of solvent are included to minimize saturation of the H_2O signal. Delays used were $\tau = 6.25$ ms and $\Delta = 2.03$ ms. The recycle delay was 1.25 s. τ was chosen such that the signals arising from Tyr $^1J_{CH}$ ^{13}C-^{1}H couplings are suppressed, i.e., τ equals a multiple of $1/(2 \times {}^1J_{CH})$ (21).

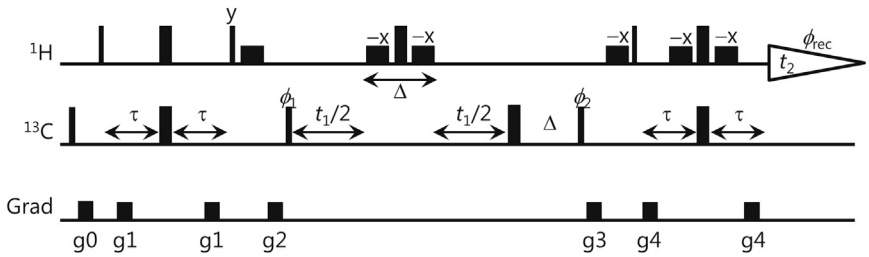

FIGURE 2 Long-range ^{1}H-^{13}C correlation experiment to assign the hydroxyl proton of Tyr-42 unambiguously. The experiment exploits the $^3J_{CH}$ (and $^2J_{CH}$) couplings between the ^{1}Hη and ^{13}Cε (and ^{13}Cζ).

Empirically, we found that, given that $^1J_{CH}$ is 160 Hz, sensitivity of the spectrum was highest when setting $\tau = 2/(2 \times 160) = 6.25$ ms. Durations of the z-axis pulsed-field gradients were 1.0 ms. The phase cycle employed was $\phi_1 = \{x, -x\}$, $\phi_2 = \{x, x, -x, -x\}$, and $\phi_{rec} = \{x, -x, -x, x\}$. Quadrature detection in the t_1 dimension was achieved with the States-TPPI protocol.

Data analysis

The chemical-shift titration data were analyzed using the Henderson-Hasselbalch equation, appropriate for rapid exchange of the nuclei between environments associated with neutral and charged states of the side chain:

$$\delta_{obs} = \delta_{AH} + \Delta\delta \frac{10^{(pH-pK_a)}}{1 + 10^{(pH-pK_a)}}, \quad (1)$$

where δ_{AH} denotes the chemical shift for the protonated form, and $\Delta\delta = \delta_A - \delta_{AH}$ is the change in chemical shift upon deprotonation. All fitting of models to data was performed using in-house routines written in Mathematica software (Wolfram Research, Champaign, IL).

RESULTS

pH-titration experiments were performed in the pH range 3.4–11.4. In this range, the protein is folded as indicated by the appearance of the ^{1}H-^{15}N heteronuclear single-quantum correlation spectrum and also by the presence of signals for the protons belonging to the two short hydrogen bonds of Tyr-42 and Glu-46 with the *p*CA chromophore (vide infra). Below pH 3, PYP is partially unfolded (30), and above pH 11.7, the thioester bond that connects the *p*CA chromophore to Cys-69 would be hydrolyzed (6).

Titration of glutamic acid and aspartic acid residues

The protonation state and pK_a constants for Glu and Asp residues are typically established by monitoring the side-chain carboxyl (^{13}Cγ/^{13}Cδ) chemical-shift changes using the 2D H2(C)CO experiment (23). However, since signals for Glu-46 and Asp-53 were not detected in the H2C(C)O spectrum, we resorted to (H)C(CO)NH-TOCSY spectroscopy to follow ^{13}C$\gamma\beta$ and ^{13}Cγ chemical shifts for Asp and Glu, respectively, based on previously established assignments (31).

As exemplified for the solvent-exposed residue Glu-74 in Fig. 3, *B* and *D*, deprotonation is typically accompanied by a change in the ^{13}Cγ chemical shift of ~4 ppm (19). Fig. 3, *A* and *C*, clearly demonstrates the absence of chemical shift changes for Glu-46 in the pH range 3.4–11.4, indicating that its protonation state stays constant over that pH interval. The ^{13}Cγ chemical-shift value is indicative of a protonated state for Glu-46. This is confirmed by direct observation of the hydroxyl resonance (vide infra).

Assignment of the Tyr-42 and Glu-46 hydrogen-bond proton signals was reported by Sigala et al. (32), based on 2D ^{1}H-^{1}H NOESY spectroscopy. In agreement with this, our previous study using water flip-back 1D ^{1}H NMR, reported the presence of two distinct proton signals at 13.55 and 15.25 ppm, which were assigned to a hydrogen-bonded proton from Tyr-42 to *p*CA and the proton shared by Glu-46 and *p*CA, respectively (31). However, since 2D ^{1}H-^{1}H NOESY was used to assign two protons, which are in very close proximity, the assignment of Tyr-42 and Glu-46 might be open to argument. Therefore, to determine the assignment of the hydroxyl proton for Tyr-42 unambiguously, we performed a long-range ^{1}H-^{13}C correlation experiment, which exploits the ^{3}J$_{CH}$ (and ^{2}J$_{CH}$) couplings between the ^{1}Hη and ^{13}Cε (and ^{13}Cζ) in tyrosine residues (21,33). The resulting spectrum is shown in Fig. 4, and it confirms the previously reported assignment of hydrogen-bonded protons from Tyr-42 and Glu-46 (31,32).

Next, using water flip-back 1D proton NMR spectroscopy, signals due to hydrogen- bonded protons from Tyr-42 and Glu-46 were monitored as a function of pH. Fig. 5 shows that these proton signals are present in the entire pH range 3.4–11.4 at 20°C. This result is consistent with our previous finding that the Tyr-42 pK_a value is >13 (24). Again, electrostatic interactions in the active site of PYP remain unaltered in the pH range 3.4–11.4 in the dark state. In addition, the chemical shifts of the hydrogen-bonded protons of Glu-46 and Tyr-42 do not change, which implies that those bonds have a very persistent geometry in the pG state over the entire pH range studied here.

The hydrogen bond to the backbone carbonyl of Thr-50 remains intact

Based on the crystal structure of PYP, the backbone carbonyl of Thr-50 participates in a hydrogen bond with Hη of Arg-52 (2). A previous study showed that backbone carbonyl chemical-shift changes can be used to probe

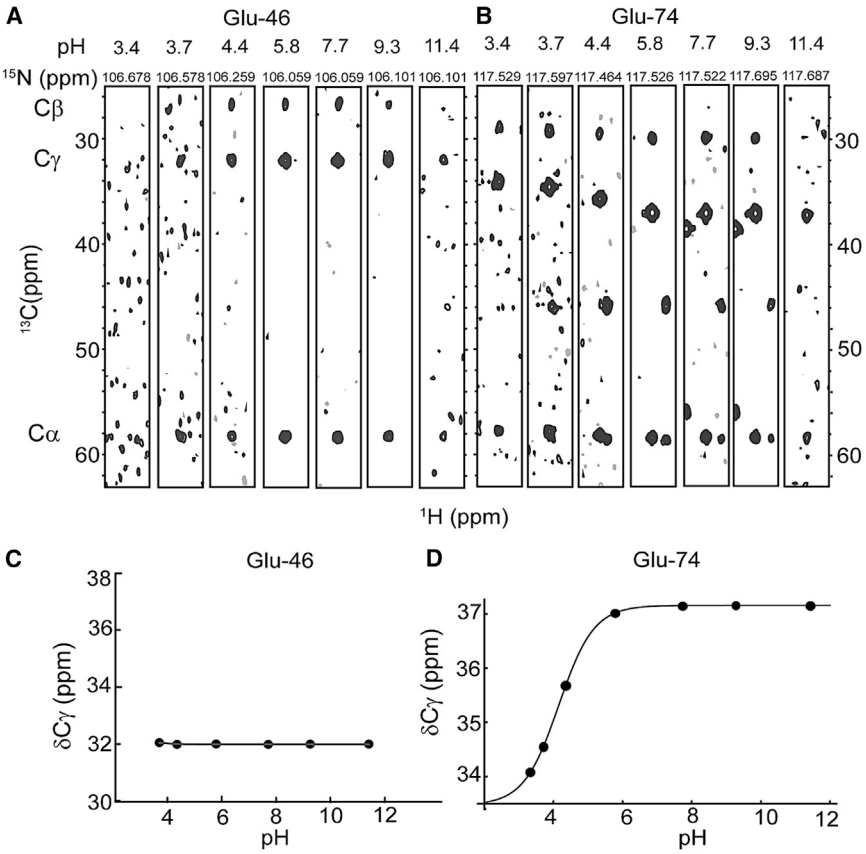

FIGURE 3 Protonation state of Glu-46 does not change over the pH range 3.4–11.4. Strip plots for Glu-46 (*A*) and Glu-74 (*B*) taken from 3D (H) C(CO)NH TOCSY spectra, and graphs of the $^{13}C\gamma$ chemical shift as a function of pH for Glu-46 (*C*) and Glu-74 (*D*).

hydrogen bonding of non-titrating residues. For example, a change of 1 ppm in backbone carbonyl ^{13}C chemical shift was observed for Lys-10 in the B1 domain of protein G, and found to accurately reflect the pK_a value of the donor Glu-56 (34).

We therefore used the pH-dependence of the Thr-50 backbone carbonyl ^{13}C chemical shift to test for any pH-dependent change in hydrogen bonding of Thr-50 to Arg-52, using 2D CO(CA)HA spectroscopy (35). This 2D NMR experiment, which correlates backbone carbonyl and Hα signals, is suitable for pH titration studies, since Hα protons do not exchange with water. As shown in Fig. 6 *A*, there is no chemical-shift change of the Thr-50 carbonyl resonance during the titration from pH 5.0 to pH 11.2. For comparison, we observe an ~0.5 ppm change in the backbone carbonyl chemical shift of Thr-70, which reports the pK_a value of Asp-71 (Fig. 6, *B* and *C*). The small (~0.2 ppm) change below pH 5 most likely reflects the onset of a large change as a result of loss of the hydrogen bond to the chromophore, which occurs below pH 3.

DISCUSSION

Lack of titration in the active site of PYP

The NMR chemical shifts of nuclei nearby titratable groups carry information about individual titratable amino acid groups in the protein. In this study, we show that the side chain of Glu-46 does not change its protonation state over the entire pH range 3.4–11.4. Our study also shows that the side chain of Tyr-42 stays protonated in the same pH range. These conclusions are supported by the existence of hydrogen bonds between Glu-46 and *p*CA and between Tyr-42 and *p*CA, as directly observed by 1D ^{1}H NMR. The lack of any chemical-shift changes also indicates that the chromophore *p*CA stays unaltered in that pH range. In addition, the side chain of Tyr-94, which forms a hydrogen bond with the backbone carbonyl of Cys-69, and Thr-50, which is hydrogen bonding to Arg-52, remains in the same protonation state in the pH range 3.4–11.4 (24). These results indicate that the active site of the PYP pG state is remarkably robust, and that all pK_a constants lie outside of the studied pH interval. What is more, changes in the chromophore protonation state may be incompatible with an energetically stable pG structure, and they lie at the basis of the existence of the pB signaling state.

Stabilization of the *p*CA chromophore

When Glu-46 and Tyr-42 are mutated, significant changes in the wavelength absorption maximum of PYP are observed (14,36). The short hydrogen bonds between the phenolic oxygen of the chromophore *p*CA and the side chains of Glu-46

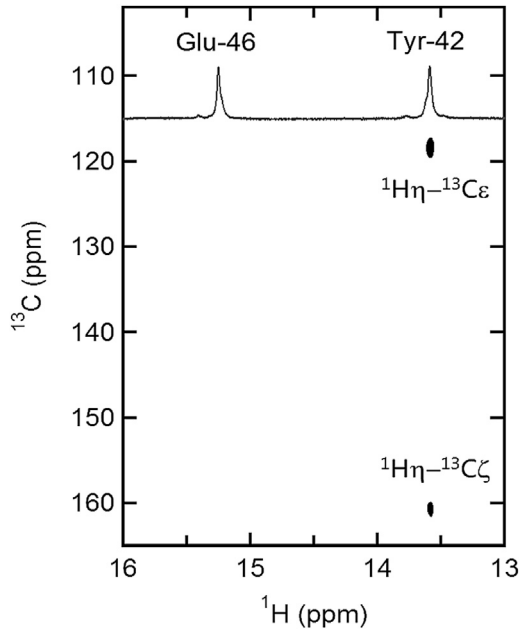

FIGURE 4 Assignment of long-range ^{1}H-^{13}C correlation of ^{1}Hη-^{13}Cε and ^{1}Hη-^{13}Cζ of Tyr-42. The 2D spectrum was obtained by conducting a long-range ^{1}H-^{13}C correlation experiment that utilizes $^{3}J_{CH}$ and $^{2}J_{CH}$ couplings between the ^{1}Hη and ^{13}Cε as well as ^{1}Hη and ^{13}Cζ in tyrosine residues. A 1D ^{1}H spectrum is shown as an insert.

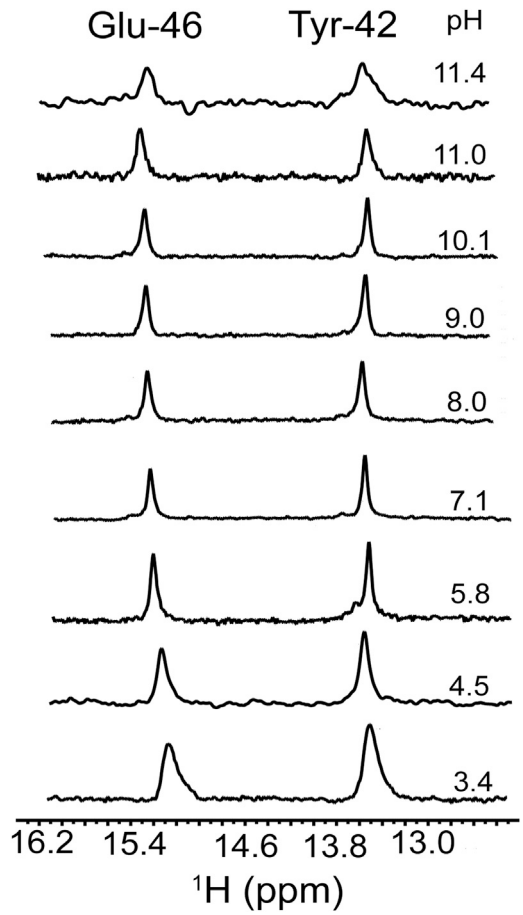

FIGURE 5 pH titration of two hydrogen-bond protons of Glu-46 and Tyr-42. 1D ^{1}H NMR spectra showing the resonances of the hydrogen-bond protons of Glu-46 and Tyr-42 from pH 3.4 to pH 11.4.

and Tyr-42 stabilize surplus electron density by redistribution over an extended conjugated network. The mutation of Glu-46 to Gln red-shifts the absorption maximum of *p*CA from 446 to 462 nm (11,26,36). This shift can be rationalized in terms of an increased negative charge density on the chromophore, since the hydrogen bond between Gln and *p*CA is weaker than that between Glu and *p*CA. A red shift in the absorption maximum (from 446 to 466 nm) is also found when PYP is reconstituted with a modified chromophore containing an electron withdrawing cyano group (32). Also, when Tyr-42 is mutated to Phe, two peaks occur in the absorption spectrum of *p*CA (at 458 and 385 nm) (36). This result demonstrates that two populations are present, which corresponds to a structural change of the *p*CA chromophore. Since the absorption at 385 nm is much closer to the absorption in the pB state, this also may indicate that some of the population may shift toward the pB state, in which the surrounding of *p*CA does not stay intact in the active site of PYP.

A recent quantum mechanics/molecular mechanics computational study suggested that the pK_a values of Glu-46 and *p*CA are 8.6 and 5.4, respectively, in the pG state (16). However, the result of this computational study is not in agreement with our experimental data, where none of the titratable groups in the active site changed their protonation state in the measured interval pH 3.4–11.4. On the other hand, a neutron crystallography study proposed similar values for the two proton affinities as a consequence of the presence of a low-barrier hydrogen bond between them (4). Apparently, the very strong electrostatic coupling between the two residues prevents their individual titration from being measured. The hydrogen bond between *p*CA and Glu-46 is so strong to keep the chromophore *p*CA locked in the active site of PYP in the dark state. Absorption of a photon by the chromophore leads to an injection of a tremendous amount of energy into the structure, being redistributed among various degrees of freedom over several timescales, finally dislodging the helix containing Tyr-42 and Glu-46 and leading to significant structural change (37,38). Tacking the helix by strong hydrogen-bonding interactions to the chromophore ensures structural stability in the dark state while maintaining the possibility of presenting a very different conformation upon light capture, and presents a remarkable solution of Nature for life to respond to light.

The pH dependence of kinetic recovery

Our study reveals that the pH dependence of pG-state recovery is not due to a protonation or deprotonation event in the pG state. Therefore, it should result from protonation-state changes in the pB state. The bell-shaped curve for the rate constant of PYP conversion to pG as a function of pH

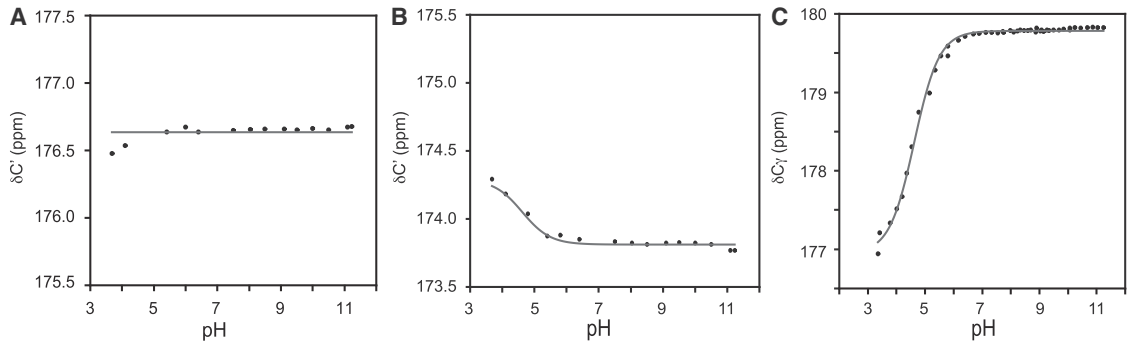

FIGURE 6 pH dependence of the backbone carbonyl ($^{13}C'$) chemical shifts of Thr-50 (*A*) and Thr-70 (*B*) and the side-chain carboxyl of Asp-71 (*C*). pH dependence of the backbone carbonyl of Thr-70 reflects the side-chain pK_a value of Asp-71 (pK_a of Asp-71 is 4.6).

reflects two *p*K constant values of 6.37 and 9.35 (14,15). Those p*K* constants would correspond well with the pK_a of Glu-46 and *p*CA in the pB state, where both groups become more solvent exposed. Our results provide direct evidence for the proposal of Demchuk et al. (15), where the pK_a value for Glu-46 is predicted to be extremely high. It also agrees with a pK_a value of 2.8 for chromophore *p*CA, based on ultraviolet-visible spectroscopy (18), although based on recent results, it is not possible to change the charge state of either group while retaining the native structure, and the proton may actually not be assigned to only one of the two groups (4). The explanation is also consistent with a second theoretical study suggesting that the pK_a values of *p*CA and Glu-46 are close to their intrinsic values of 9.0 and 4.3, respectively, in the pB state (15). Following Demchuk et al. (15), the fraction of pB that is productive in the forward reaction to pG is shown in Fig. 7, calculated based on Eq. 2, below, which is the product of the productive-protonation-state fraction as a function of pH, namely, protonated Glu-46 and deprotonated *p*CA:

$$F = \frac{1}{(1+10^{pH-pK_1})} \times \frac{1}{(1+10^{pK_2-pH})} \qquad (2)$$

where pK_1 is 6.4 and pK_2 is 9.4. The pK_a constants are assigned to the side chain of Glu-46 and to *p*CA, respectively,

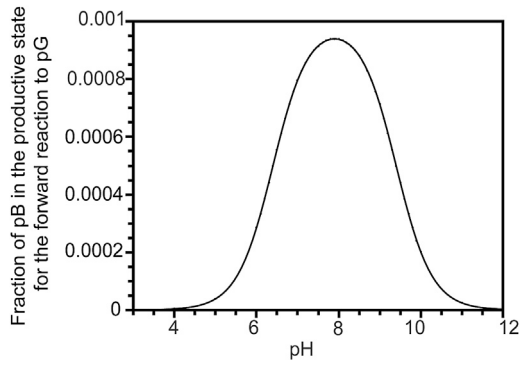

FIGURE 7 The fraction of the pB state that helps produce the return to the pG state, as a function of pH.

in the pB state, as suggested previously (15). These pK_a values are somewhat shifted relative to the pK_a values for a solvent-exposed Glu side chain (4.3) and *p*CA (9.0). A 2.1 unit difference between the pK_a value of a solvent-exposed Glu side chain and that obtained in the pB state, and a 0.4 unit change for *p*CA might arise from the fact that these groups are not completely solvent exposed in pB and hence experience a reduced dielectric constant. Also, hydrogen bonds donated by Glu-46 in the pB state could contribute to such a shift. As a high-resolution structure of full-length PYP in the pB state in solution is not available, these hypotheses cannot be verified at present.

A model can be envisaged where obtaining the correct protonation state is a prerequisite for returning to the pG state and precedes the rate-limiting step of *cis*-to-*trans* conversion of the chromophore double bond. In such a scenario, the concentration of the productive state for the forward reaction could then be calculated from knowledge of the acidity constants of the two residues in both states. As we have demonstrated here, the pK_a constants for Glu-46 and *p*CA in pG lie far outside the physiological pH window, such that these can be considered constant. The protonation equilibria in pB would then dominate pG-state recovery. Fig. 7 shows the fraction of pB that is in the productive state for the forward reaction to pG. The low population of this state would directly contribute to the observed very slow process of recovery, which occurs on a timescale of seconds. This line of argumentation also explains that, when Glu-46 is substituted by Gln, different kinetics are observed. Below pH 7, the recovery rate is still slow but almost two orders of magnitude faster than the optimum of the wild-type kinetics at high pH (14), as Gln can donate a hydrogen bond to *p*CA at any pH such that pG recovery becomes a lot faster and now only depends on the probability that *p*CA is deprotonated (7,39).

CONCLUSIONS

In sum, we provide here a pK_a determination for the active-site side chains of PYP using NMR spectroscopy. Our study shows that there are no chemical-shift changes observed for the active-site residues in the pH range 3.4–11.4,

demonstrating that the pG state of PYP is completely insensitive to pH in the region where the protein is chemically and structurally stable. This result is supported by the fact that Tyr-42 and Glu-46 hydrogen-bond proton signals are also observed in the same pH range. Our experimental results conclusively establish that the pH-dependent pG-state recovery kinetics must be due to protonation events in the pB state. Our results are consistent with the view that return to the pG state requires two mutually opposing pH-dependent events, deprotonation of the chromophore and protonation of Glu-46.

SUPPORTING MATERIAL

One table is available at http://www.biophysj.org/biophysj/supplemental/S0006-3495(17)30396-X.

REFERENCES

1. Sprenger, W. W., W. D. Hoff, …, K. J. Hellingwerf. 1993. The eubacterium *Ectothiorhodospira halophila* is negatively phototactic, with a wavelength dependence that fits the absorption spectrum of the photoactive yellow protein. *J. Bacteriol.* 175:3096–3104.
2. Borgstahl, G. E., D. R. Williams, and E. D. Getzoff. 1995. 1.4 Å structure of photoactive yellow protein, a cytosolic photoreceptor: unusual fold, active site, and chromophore. *Biochemistry.* 34:6278–6287.
3. Düx, P., G. Rubinstenn, …, R. Kaptein. 1998. Solution structure and backbone dynamics of the photoactive yellow protein. *Biochemistry.* 37:12689–12699.
4. Yamaguchi, S., H. Kamikubo, …, M. Kataoka. 2009. Low-barrier hydrogen bond in photoactive yellow protein. *Proc. Natl. Acad. Sci. USA.* 106:440–444.
5. Baca, M., G. E. Borgstahl, …, E. D. Getzoff. 1994. Complete chemical structure of photoactive yellow protein: novel thioester-linked 4-hydroxycinnamyl chromophore and photocycle chemistry. *Biochemistry.* 33:14369–14377.
6. Hoff, W. D., B. Devreese, …, K. J. Hellingwerf. 1996. Chemical reactivity and spectroscopy of the thiol ester-linked *p*-coumaric acid chromophore in the photoactive yellow protein from *Ectothiorhodospira halophila*. *Biochemistry.* 35:1274–1281.
7. Kim, M., R. A. Mathies, …, K. J. Hellingwerf. 1995. Resonance Raman evidence that the thioester-linked 4-hydroxycinnamyl chromophore of photoactive yellow protein is deprotonated. *Biochemistry.* 34:12669–12672.
8. Genick, U. K., G. E. Borgstahl, …, E. D. Getzoff. 1997. Structure of a protein photocycle intermediate by millisecond time-resolved crystallography. *Science.* 275:1471–1475.
9. Kort, R., H. Vonk, …, K. J. Hellingwerf. 1996. Evidence for *trans-cis* isomerization of the *p*-coumaric acid chromophore as the photochemical basis of the photocycle of photoactive yellow protein. *FEBS Lett.* 382:73–78.
10. van der Horst, M. A., I. H. van Stokkum, …, K. J. Hellingwerf. 2001. The role of the N-terminal domain of photoactive yellow protein in the transient partial unfolding during signalling state formation. *FEBS Lett.* 497:26–30.
11. Brudler, R., T. E. Meyer, …, E. D. Getzoff. 2000. Coupling of hydrogen bonding to chromophore conformation and function in photoactive yellow protein. *Biochemistry.* 39:13478–13486.
12. Hendriks, J., and K. J. Hellingwerf. 2009. pH Dependence of the photoactive yellow protein photocycle recovery reaction reveals a new late photocycle intermediate with a deprotonated chromophore. *J. Biol. Chem.* 284:5277–5288.
13. Imamoto, Y., M. Harigai, and M. Kataoka. 2004. Direct observation of the pH-dependent equilibrium between L-like and M intermediates of photoactive yellow protein. *FEBS Lett.* 577:75–80.
14. Genick, U. K., S. Devanathan, …, E. D. Getzoff. 1997. Active site mutants implicate key residues for control of color and light cycle kinetics of photoactive yellow protein. *Biochemistry.* 36:8–14.
15. Demchuk, E., U. K. Genick, …, D. Bashford. 2000. Protonation states and pH titration in the photocycle of photoactive yellow protein. *Biochemistry.* 39:1100–1113.
16. Saito, K., and H. Ishikita. 2012. Energetics of short hydrogen bonds in photoactive yellow protein. *Proc. Natl. Acad. Sci. USA.* 109:167–172.
17. Kroon, A. R., W. D. Hoff, …, K. J. Hellingwerf. 1996. Spectral tuning, fluorescence, and photoactivity in hybrids of photoactive yellow protein, reconstituted with native or modified chromophores. *J. Biol. Chem.* 271:31949–31956.
18. Philip, A. F., K. T. Eisenman, …, W. D. Hoff. 2008. Functional tuning of photoactive yellow protein by active site residue 46. *Biochemistry.* 47:13800–13810.
19. Hass, M. A. S., and F. A. A. Mulder. 2015. Contemporary NMR studies of protein electrostatics. *Annu. Rev. Biophys.* 44:53–75.
20. André, I., S. Linse, and F. A. A. Mulder. 2007. Residue-specific pKa determination of lysine and arginine side chains by indirect ^{15}N and ^{13}C NMR spectroscopy: application to apo calmodulin. *J. Am. Chem. Soc.* 129:15805–15813.
21. Baturin, S. J., M. Okon, and L. P. McIntosh. 2011. Structure, dynamics, and ionization equilibria of the tyrosine residues in *Bacillus circulans* xylanase. *J. Biomol. NMR.* 51:379–394.
22. Hass, M. A. S., A. Yilmaz, …, J. J. Led. 2009. Histidine side-chain dynamics and protonation monitored by ^{13}C CPMG NMR relaxation dispersion. *J. Biomol. NMR.* 44:225–233.
23. Oda, Y., T. Yamazaki, …, H. Nakamura. 1994. Individual ionization constants of all the carboxyl groups in ribonuclease HI from *Escherichia coli* determined by NMR. *Biochemistry.* 33:5275–5284.
24. Oktaviani, N. A., T. J. Pool, …, F. A. A. Mulder. 2012. Comprehensive determination of protein tyrosine pK_a values for photoactive yellow protein using indirect ^{13}C NMR spectroscopy. *Biophys. J.* 102:579–586.
25. Yoshimura, Y., N. A. Oktaviani, …, F. A. A. Mulder. 2017. Unambiguous determination of protein arginine ionization states in solution by NMR spectroscopy. *Angew. Chem. Int. Ed. Engl.* 56:239–242.
26. Mihara, K., O. Hisatomi, …, F. Tokunaga. 1997. Functional expression and site-directed mutagenesis of photoactive yellow protein. *J. Biochem.* 121:876–880.
27. Delaglio, F., S. Grzesiek, …, A. Bax. 1995. NMRPipe: a multidimensional spectral processing system based on UNIX pipes. *J. Biomol. NMR.* 6:277–293.
28. Goddard, T., and D. Kneller. 2003. SPARKY 3. University California, San Fransisco.
29. Markley, J. L., A. Bax, …, K. Wüthrich. 1998. Recommendations for the presentation of NMR structures of proteins and nucleic acids—IUPAC-IUBMB-IUPAB Inter-Union Task Group on the standardization of data bases of protein and nucleic acid structures determined by NMR spectroscopy. *Eur. J. Biochem.* 256:1–15.
30. Craven, C. J., N. M. Derix, …, R. Kaptein. 2000. Probing the nature of the blue-shifted intermediate of photoactive yellow protein in solution by NMR: hydrogen-deuterium exchange data and pH studies. *Biochemistry.* 39:14392–14399.
31. Pool, T. J., N. A. Oktaviani, …, F. A. A. Mulder. 2013. ^{1}H, ^{13}C, and ^{15}N resonance assignment of photoactive yellow protein. *Biomol. NMR Assign.* 7:97–100.
32. Sigala, P. A., M. A. Tsuchida, and D. Herschlag. 2009. Hydrogen bond dynamics in the active site of photoactive yellow protein. *Proc. Natl. Acad. Sci. USA.* 106:9232–9237.
33. Werner, M. H., G. M. Clore, …, A. M. Gronenborn. 1997. Correction of the NMR structure of the ETS1/DNA complex. *J. Biomol. NMR.* 10:317–328.

34. Lindman, S., S. Linse, …, I. André. 2007. pK_a values for side-chain carboxyl groups of a PGB1 variant explain salt and pH-dependent stability. *Biophys. J.* 92:257–266.

35. Dijkstra, K., G. J. A. Kroon, …, R. M. Scheek. 1994. The COCAH experiment to correlate intraresidue carbonyl, Cα, and Hα resonances in proteins. *J. Magn. Reson. A.* 107:102–105.

36. Imamoto, Y., H. Koshimizu, …, F. Tokunaga. 2001. Roles of amino acid residues near the chromophore of photoactive yellow protein. *Biochemistry.* 40:4679–4685.

37. Rubinstenn, G., G. W. Vuister, …, R. Kaptein. 1998. Structural and dynamic changes of photoactive yellow protein during its photocycle in solution. *Nat. Struct. Biol.* 5:568–570.

38. Tamiola, K., and F. A. A. Mulder. 2012. Using NMR chemical shifts to calculate the propensity for structural order and disorder in proteins. *Biochem. Soc. Trans.* 40:1014–1020.

39. Anderson, S., S. Crosson, and K. Moffat. 2004. Short hydrogen bonds in photoactive yellow protein. *Acta Crystallogr. D Biol. Crystallogr.* 60:1008–1016.